Spectroscopic and Theoretical Study on Isomerism, Prototautomerism, and Acid Dissociation Constants of 2-Hydroxy-3-(3-oxo-1-phenylbutyl)chromen-4-one

Cemil Öğretir,*,† Sinem Aydemir,‡ Murat Duran,† and M. Selami Kılıçkaya‡

Department of Chemistry and Department of Physics, Faculty of Arts & Science, Eskişehir Osmangazi University, 26480 Eskişehir, Turkey

The prototropic, tautomeric, and ionization equilibria of all of the structures of 2-hydroxy-3-(3-oxo-1-phenylbutyl)chromen-4-one (warfarin) were studied experimentally and theoretically. The structure elucidation and acidity constant determination along with the tautomeric equilibrium constants were carried out experimentally by a UV−visible spectroscopic method and theoretically investigated at the HF/6-31G(d) and B3LYP/6-31G(d) levels of theory. The obtained K_a values were evaluated by structure elucidation and a protonation mechanism. Using the gauge-including atomic-orbital (GIAO) method for calculating ^{1}H and ^{13}C nuclear magnetic shielding tensors, the Hartree−Fock (HF) and density functional (DFT) levels of theory were applied to warfarin. Geometry optimizations were also performed on each species, and the absence of negative frequencies verified that all structures were true minima. Theoretical values were compared to the experimental data. Satisfactory agreement between the experimental chemical shifts and the theoretical values of shielding constants (calculated by GIAO/DFT and GIAO/HF methods) was obtained.

Introduction

Warfarin is a widespread anticoagulant used in medicine to prevent strokes. Racemic warfarin [3-α-(acetonylbenzyl)-4-hydroxycoumarin], a synthetic 4-hydroxycoumarin derivative and vitamin K antagonist,[1] has been utilized for more than two decades as an oral anticoagulant (OA) and as a rodenticide. The OA warfarin [4-hydroxy-3-(L-phenyl-3-oxobutyl)-2*H*-l-benzopyran-2-one] has found extensive clinical use in the treatment of such pathological conditions as thrombophlebitis, pulmonary emboli, and myocardial infarction.[2] Warfarin has been synthesized by the Michael addition of 4-hydroxycoumarin to benzylacetone under a number of acid- or base-catalyzed conditions.[3] Warfarin is usually named and depicted as an open tautomer, although the molecular form in the crystalline state is the cyclic tautomer, the hemiketal. Therefore, carbon numbering and the chemical name of the cyclic form for warfarin should be 2-hydroxy-3-(3-oxo-1-phenylbutyl)chromen-4-one (Figure 1).

Earlier results suggest[4–7] that the active form of warfarin is the hydrogen-bonded eight-membered cyclic ring structure. Although the structure of warfarin is usually drawn as an open chain structure, this is not the only possible form of this drug. Warfarin is generally thought to exist in solution as a cyclic hemiketal;[8] this same form has been observed in warfarin crystals.[9,10]

We now report on the usefulness of combined solid-state NMR and theoretical approaches to obtain information on the structure of coumarin anticoagulants in the solid phase and to determine the acidity constants, respectively. Acid dissociation constants, pK_a values, are important parameters to denote the extent of ionization of a molecule in solution at different pH values.[11] If a sample is sufficiently soluble in a water−ethanol mixed solvent, it is possible to determine pH-metrically the apparent pK_a in cosolvent mixtures.[12] Dissociation constants of a substance can be determined by different methods. Potentiometric, chromatographic, and electrophoretic methods have been used widely. Further, a method based on spectrophotometry has been used widely by the help of improved computer programs.[13–15] The determination of the ionization constant by UV−vis spectrophotometry is an ideal method when a substance is too

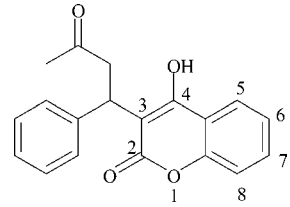

Figure 1. Structure of 2-hydroxy-3-(3-oxo-1-phenylbutyl)chromen-4-one (warfarin).

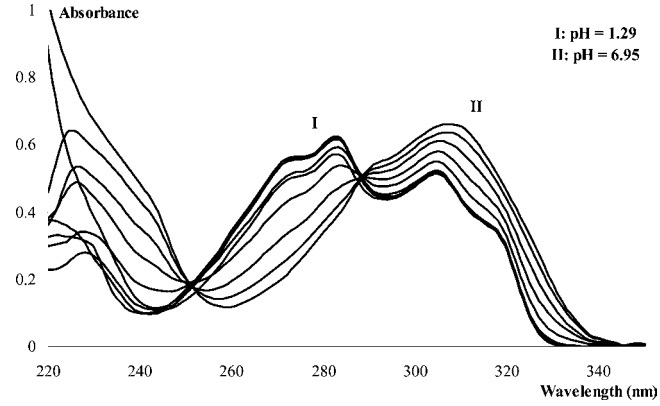

Figure 2. Spectral changes of warfarin at various pH conditions, between (220 and 340) nm.

* Corresponding author. Tel.: +90 222 239 37 50/2873. Fax: +90 222 239 35 78. E-mail: cogretir@ogu.edu.tr.
† Department of Chemistry. E-mail: mduran@ogu.edu.tr (M.D.).
‡ Department of Physics. E-mail: saydemir@ogu.edu.tr (S.A.); selamik@ogu.edu.tr (M.S.K.).

10.1021/je900456v
Published on Web 03/03/2010

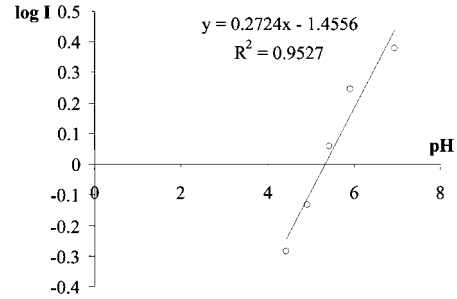

Figure 3. pH as a function of log *I* (at 270 nm), plot for the protonation of the molecule warfarin.

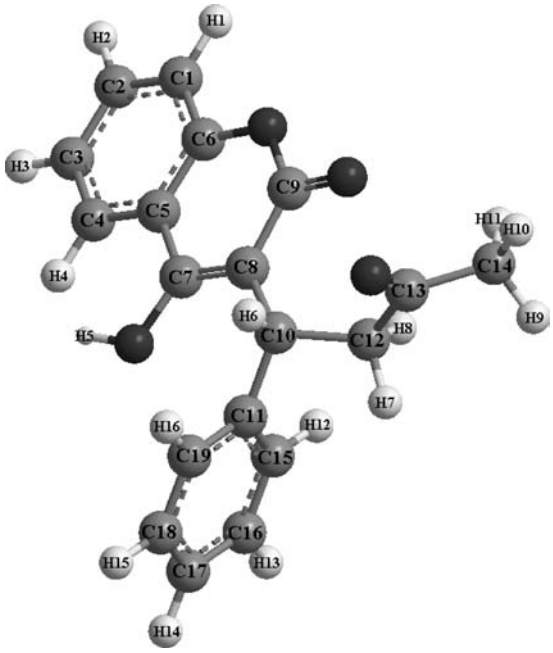

Figure 4. Numbering system of 2-hydroxy-3-(3-oxo-1-phenylbutyl)chromen-4-one (warfarin) for ^{1}H NMR and ^{13}C NMR tables.

insoluble for potentiometry or when its pK_a value is particularly low or high.[16] It is known that, in general, spectroscopic methods are highly sensitive and suitable for studying chemical equilibria solutions. These methods involve the direct determinations of the mole ratio of acid−base conjugate pairs in a series of buffered solutions of known pH. If the components involved in the equilibrium can be obtained in pure form and if their spectral responses do not overlap, the analysis is very simple.[17]

As a continuation of our previous study of warfarin, we extended our studies to nuclear shielding calculations. We have used several theoretical methods and conclusively identified the density functional theory (DFT) and the Hartree−Fock (HF) approach for ^{1}H and ^{13}C NMR chemical shifts.

Experimental Section

Materials and Solutions. The structure and nomenclature of warfarin are shown in Figure 1. All reagents were spectroscopic grade and not further purified.

The buffer solutions employed were prepared from the following: (a) HCl−KCl, pH = 1; (b) KH_2PO_4−NaOH, pH = 7.0; (c) Borax−HCl, pH = 8.0 to 9.0; (d) Borax−NaOH, pH = 9.3 to 10.7; and (e) Na_2HPO_4−NaOH, pH = 10.9 to 11.5, as described in the literature.[18]

Equipment. The pH values were measured by a pH/ion analyzer (Orion 720 A+ pH meter) which is furnished with a combined glass electrode standardized at 25 °C by using standard buffers of pH 4, 7, and 9. The UV−vis spectra, obtained to determine the pK_a values, were recorded at each pH using a Hitachi 150-20 double beam spectrophotometer controlled by a computer and equipped with a 1 cm path length quartz cell. After each pH adjustment, the solution is transferred into a cuvette, and the absorption spectra are recorded. Spectra were acquired between (220 and 340) nm (1 nm resolution) (Figure 2).

Scheme 1. Thermodynamic Cycle Illustrating the Calculation of Theoretical pK_a values

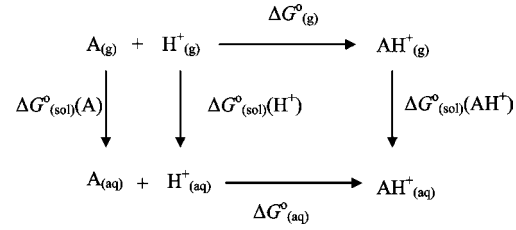

Procedures. A stock solution of 0.001 M 2-hydroxy-3-(3-oxo-1-phenylbutyl)chromen-4-one was prepared in a mixed solvent of 1:1 ethanol−water. Sample solutions were prepared by adding 0.50 mL of stock solution to 9.5 mL of buffer solution and a series of 10 mL volumetric flasks were obtained. In this way, the sample solutions which have absorbance values between 0.5 and 1.0 were prepared. The optical density of each solution was then measured in 1.0 cm cells, against solvent blanks, using a constant temperature cell-holder in the spectrophotometer.

The spectrophotometer was thermostatted at 25 °C (to within ± 0.1 °C). The wavelengths were chosen such that the fully protonated form of the substrate had a very much greater or very much smaller extinction coefficient than the neutral form. The calculation was carried out as follows: the sigmoid curve of the optical density against pH at the analytical wavelength (OD_{obs}, λ_{max}) was obtained first. The optical densities of the fully protonated molecule (OD_{ca}; optical density of conjugated acid) and the pure free base (OD_{fb}; optical density of free base), at a pH where the substrate is in a partially protonated form, were then calculated by linear extrapolation of the arms of the curve.

Procedure for Spectrophotometric Measurement. Determination of Acidity Constants. As stated earlier, spectrophotometry is an ideal method when a substance is not soluble enough for potentiometry or when its pK_a value is particularly low or high (e.g., less than 2 or more than 11). The method depends on the direct determination of the ratio of the molecular species in a series of nonabsorbing buffer solutions for which pH values are either known or measured. For a weak base B which ionizes by simple proton addition the pH values at half-protonation were measured for the studied molecules during the course of the present work, using the UV spectrophotometric method of Johnson.[17] This method takes into account any medium effect on the wavelength of the maximum UV absorption and the corresponding extinction coefficient.

The ionization ratio is given by eq 1, where the OD_{obs} (observed optical density) is the measured optical density of the solution at the analytical wavelength;

$$I = \frac{[BH^+]}{[B]} = \frac{(OD_{obs} - OD_{fb})}{(OD_{ca} - OD_{obs})} = \frac{\varepsilon_{obs} - \varepsilon_{fb}}{\varepsilon_{ca} - \varepsilon_{obs}} \qquad (1)$$

where BH^+ is the protonated base, B is unprotonated (neutral) base, ε_{obs} is the observed molar extinction coefficient, ε_{fb} is the molar extinction coefficient of the free base, and ε_{ca} is the molar

Scheme 2. Possible Protonation/Deprotonation Patterns for 2-Hydroxy-3-(3-oxo-1-phenylbutyl)chromen-4-one (Warfarin)

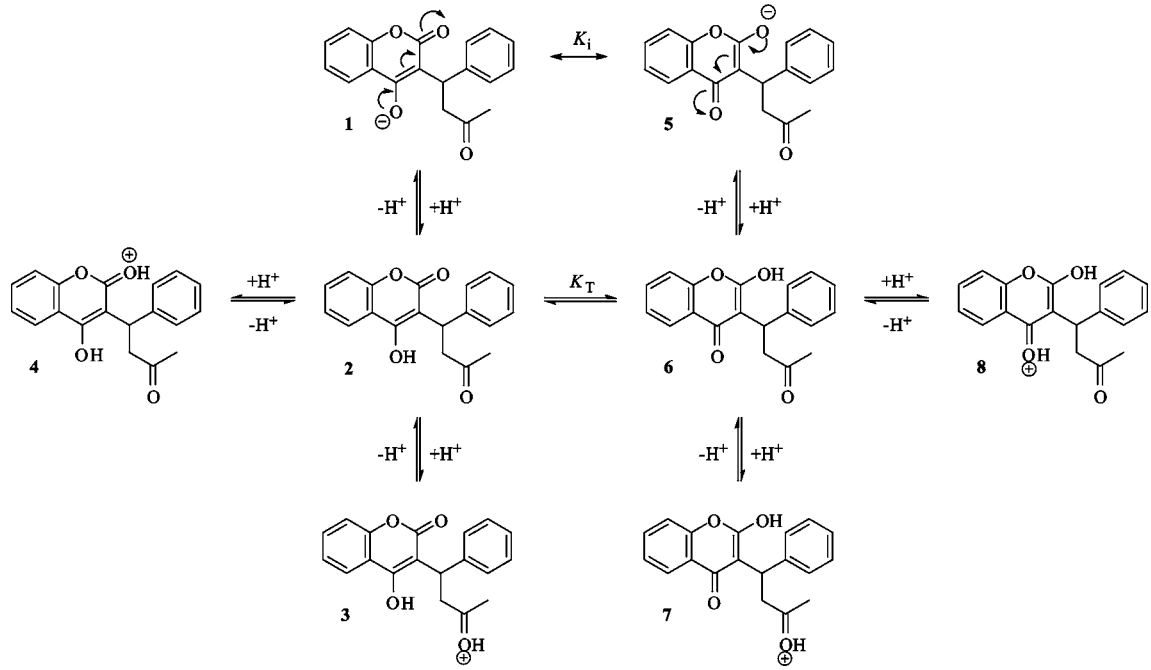

Table 1. For Neutral and Protonated Forms, Calculated Free Energies, $G_{(g)}$ and $G_{(aq)}$, Using DFT (B3LYP/6-31G(d))[a]

process	gas-phase free energy		thermal free energy (aqua phase)		solvation free energy[b] (CPCM)	
protonation	$G_{(g)}$(A)	$G_{(g)}$(AH^+)	$G_{(aq)}$(A)	$G_{(aq)}$(AH^+)	$\Delta G^o_{(sol)}$(A)	$\Delta G^o_{(sol)}$ (AH^+)
2 ⇌ 3	−2715562.23	−2716441.81	−2715628.07	−2716679.48	149140.67	−41311.72
2 ⇌ 4	−2715562.23	−2716488.97	−2715628.07	−2716693.86	128576.24	−41311.72
6 ⇌ 7	−2715547.06	−2716422.45	−2715609.08	−2716651.58	143784.56	−38922.80
6 ⇌ 8	−2715547.06	−2716483.36	−2715609.08	−2716697.52	134388.72	−38922.80
1 ⇌ 2	−2715562.23	−2714225.72	−2715628.07	−2714443.45	−136631.03	−41299.11
5 ⇌ 6	−2715547.06	−2714227.13	−2715609.08	−2716651.58	−136132.18	−38909.91

[a] Calculated from eq 4. All values are given in atomic units, hartree (1 hartree = 2625.5 kJ·mol^{-1}). [b] Solvation energies were calculated with CPCM and performed in Gaussian 03W.

Table 2. For Neutral and Protonated Forms, Calculated Free Energies, $G_{(g)}$ and $G_{(aq)}$, Using HF (HF/6-31G(d))[a]

process	gas-phase free energy		thermal free energy (aqua phase)		solvation free energy[b] (CPCM)	
protonation	$G_{(g)}$(A)	$G_{(g)}$(AH^+)	$G_{(aq)}$(A)	$G_{(aq)}$(AH^+)	$\Delta G^o_{(sol)}$(A)	$\Delta G^o_{(sol)}$(AH^+)
2 ⇌ 3	−2699004.74	−2699889.16	−2699032.75	−2700160.76	170421.21	−17564.59
2 ⇌ 4	−2699004.74	−2699939.90	−2699032.75	−2700168.89	143693.62	−17564.59
6 ⇌ 7	−2699007.58	−2699871.55	−2699083.41	−2700126.26	159840.45	−47574.06
6 ⇌ 8	−2699007.58	−2700518.25	−2699083.41	−2701215.36	43743.45	−47574.06
1 ⇌ 2	−2699004.74	−2697673.75	−2699032.75	−2697914.41	−151018.77	−17564.59
5 ⇌ 6	−2699007.58	−2697675.39	−2699083.41	−2697913.91	−149679.76	−47574.06

[a] Calculated from eq 4. All values are given in atomic units, hartree (1 hartree = 2625.5 kJ·mol^{-1}). [b] Solvation energies were calculated with CPCM and performed in Gaussian 03W.

extinction coefficient of conjugated acid (protonated species).

A linear plot of log I against pH, using the values $-1.0 < \log I < 1.0$, had a slope of m and yielded the half-protonation $H^{1/2}$ at log $I = 0$ (Figure 3) as defined in eq 3.

$$\log I = m[\mathrm{pH} - \mathrm{pH}^{1/2}] \quad (2)$$

The pK_a values were calculated by using eq 2.

$$\mathrm{p}K_a = m \cdot \mathrm{pH}^{1/2} \quad (3)$$

In the pH region studied, however, the m values are irrelevant so only the half protonation values were used.[12]

Computational Methods and Procedure. Figure 4 shows the structure of 2-hydroxy-3-(3-oxo-1-phenylbutyl)chromen-4-one and the practical numbering system adopted for the calculations performed.

Table 3. pK_a (= Half Protonation) Values of Protonation Processes

process	pK_a(calc.)		
protonation	DFT (B3LYP/6-31G(d))	HF (6-31G(d))	pK_a (expt.)
2 ⇌ 3	5.40	6.59	5.34
2 ⇌ 4	7.92	6.99	
6 ⇌ 7	4.63	7.33	
6 ⇌ 8	10.55		
1 ⇌ 2	8.04	8.95	
5 ⇌ 6	9.64	9.00	

Energies and frequencies of warfarin anions or cations were calculated using DFT, which has been a reliable technique for the calculation of molecular properties and energetics. The initial geometries of the molecules were modeled by the HF and DFT calculations. Initial estimates for the geometries of all of the structures were generated using CS Chem3D.[19] These geometries were optimized with the Gaussian 03[20] program packages,

Table 4. Isomerization K_i[a] and Tautomerization K_T[b] Constants for Studied Molecule

	K_i (DFT/6-31G(d))	K_i (HF/6-31G(d))	K_T (DFT/6-31G(d))	K_T (HF/6-31G)d))
process	isomerization		tautomerization	
1 ⇌ 5	$2.5 \cdot 10^{-2}$ ($pK_i = 1.6$)	1.12 ($pK_i = -0.05$)		
2 ⇌ 6			0.69 ($pK_T = 0.16$)	5.5 ($pK_T = -0.74$)

[a] K_i values calculated by using $K_i = K_a$(product)/pK_a (reactant). [b] K_T values calculated by using $K_T = K_a$(product)/pK_a (reactant). The positive values of pK_i and pK_T values are indicative of the predominance of the reactants.

Table 5. Calculated Optimized Geometric Parameters (Selected Bond Distance, Angles, and Dihedral Angles) of the 2-Hydroxy-3-(3-oxo-1-phenylbutyl)chromen-4-one (Warfarin) for the HF/6-31G(d)

molecules	2	3	4	6	7	8
			Bond Distance (Å)			
C1−O2	1.2149	1.1968	1.2859	1.2071	1.2146	1.291
C6−O3	1.2207	1.2589	1.1897	1.1943	1.2617	1.202
			Bond Angles (deg)			
O1−C1−C2	117.61	119.12	124.39	115.68	116.24	120.85
O3−C6−C7	116.03	121.89	116.39	117.72	122.23	117.27
			Bihedral Angles (deg)			
C1−C2−C3−C4	147.13	−162.43	−71.63	39.84	21.84	−51.21

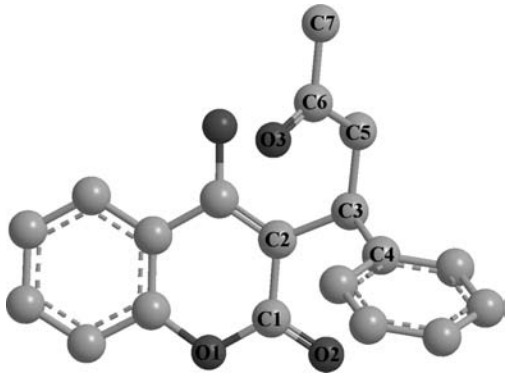

Figure 5. HF/6-31G(d) and DFT/6-31G(d) optimized structure of 2-hydroxy-3-(3-oxo-1-phenylbutyl)chromen-4-one (warfarin).

using the B3LYP function with the 6-31G(d) basis set and the default convergence criteria. To analyze for solvent effects on all of the species involved in the proposed ionization reactions, the conductor-like polarizable continuum model (CPCM)[21] was used. The obtained acidity constants are depicted in Table 3. Both HF/6-31G(d) and B3LYP/6-31G(d) methods reproduced very similar data, and both seem to be successful in describing the true value when the experimental values are taken as a reference. An excellent correlation between experimental and HF/6-31G(d) and B3LYP/6-31G(d) calculated pK_a values was observed.

On the other hand, the experimental and theoretical investigations of the 2-hydroxy-3-(3-oxo-1-phenylbutyl)chromen-4-one molecule have been performed successfully by using NMR and quantum chemical calculations. The application of the gauge-including atomic-orbital (GIAO) method yields ^{1}H and ^{13}C chemical shifts that are in reasonable agreement with experimental chemical shifts. The geometry of warfarin has been optimized by using the HF and DFT/B3LYP methods in conjunction with the 6-31G(d), 6-31+G(d), 6-31G(d,p), and 6-311+G(d,p) basis sets. After optimization, ^{1}H and ^{13}C NMR chemical shifts (δ) were calculated for warfarin using the GIAO method[22] with the B3LYP/6-31G(d), B3LYP/6-31G+(d,p), B3LYP/6-311++G(d,p), B3LYP/6-311+G(2d,p), B3LYP/6-311+G(d,p), and B3LYP/6-31G+(2d,2p) basis sets and the HF method with the same basis sets. Relative chemical shifts were then estimated by using the corresponding TMS (tetramethylsilane) shielding, calculated in advance at the same theoretical level as the reference. The molecular geometry was restricted; all of the calculations were performed by using the Gaussian 03 program package, and the GaussView program was used for molecular visualization.[19,20] The NMR chemical shifts were computed with the Becke-3-Lee−Yang−Parr (B3LYP) basis set and HF with different basis sets using the GIAO method and are given relative to that of the calculated TMS shifts at the same level of theory included in Tables 7 and 8, respectively. The GIAO ^{1}H and ^{13}C chemical shifts provide a reasonable reproduction of the experimental data.

General Scheme to Compute Absolute pK_a Values. Thermodynamic Cycle. Several authors have developed approaches for the computational determination of pK_a which involve the use of a thermodynamic cycle relating pK_a to the gas-phase proton basicity via the solvation energies ($\Delta G^o_{(sol)}$) of the products and the reactants (Scheme 1).

Inter- and intramolecular interactions can cause substantial changes in the geometry and electronic structure of compounds in solution in comparison with the isolated gas phase. Therefore, aqueous phase calculations are essential for pK_a determination, and for this reason both the Onsager and the polarizable continuum model (PCM) solvation methods have been included in the present calculations.[23] The calculation of the pK_a of a molecule, A, involves quantum mechanical calculations to characterize the gas-phase system $\Delta G^o_{(g)}$ for both the associated acid, $AH^+_{(g)}$, and the dissociated species, $H^+_{(g)}$ and $A_{(g)}$, and to characterize the solvated system ($\Delta G^o_{(aq)}$) for the associated [$AH^+_{(aq)}$] and dissociated [$H^+_{(aq)}$ and $A_{(aq)}$] species. Thus, the pK_a of $A_{(aq)}$ is given by

$$pK_a = \Delta G^o_{(aq)}/2.303RT \quad (4)$$

$$pK_a = \frac{1}{2.303RT}(\Delta G^o_{(g)} + \Delta G^o_{(sol)}(AH^+) - \Delta G^o_{(sol)}(A) - \Delta G^o_{(sol)}(H^+))$$

where

$$\Delta G^{o}_{(g)} = \Delta G^{o}_{(g)}(AH^{+}) - \Delta G^{o}_{(g)}(H^{+}) - \Delta G^{o}_{(g)}(A)$$

$$\Delta G^{o}_{(aq)} = (\Delta G^{o}_{(g)} + \Delta G^{o}_{(sol)}(AH^{+}) - \Delta G^{o}_{(sol)}(A) - \Delta G^{o}_{(sol)}(H^{+}))$$

Most of the terms in this equation will be taken from our computations, but there are two terms that need careful consideration: the free energy of a proton in the gaseous phase $\Delta G^{o}_{(g)}(H^{+})$ and its solvation free energy $\Delta G^{o}_{(sol)}(H^{+})$. In the case of the free energy of a proton in the gaseous phase, it can be easily calculated by the Sackur−Tetrode equation,[24]

$$\Delta G^{o}_{(g)}(H^{+}) = 2.5RT - T\Delta S = -26.28\ \text{kJ}\cdot\text{mol}^{-1} \quad (5)$$

Regardless which procedure is used for absolute pK_a computation, knowledge of the proton solvation energy $\Delta G^{o}_{(sol)}(H^{+})$ is required. For $\Delta G^{o}_{(g)}(H^{+})$ the experimental value of −26.28 kJ·mol^{-1} is used. Measurements of proton solvation energy $\Delta G^{o}_{(sol)}(H^{+})$ range from (−1056.88 to −1136.79) kJ·mol^{-1}.[25] In the current work, we have used the values $\Delta G^{o}_{(g)}(H^{+}) = -26.28$ kJ·mol^{-1} and $\Delta G^{o}_{(sol)}(H^{+}) = -1129.68$ kJ·mol^{-1}. The calculation of $\Delta G^{o}_{(g)}$ uses a reference state of 1 atm, and the calculation of $\Delta G^{o}_{(sol)}$ uses a 1 M reference state. Converting

Table 6. Calculated Optimized Geometric Parameters (Selected Bond Distance, Angles, and Dihedral Angles) of the 2-Hydroxy-3-(3-oxo-1-phenylbutyl)chromen-4-one (Warfarin) for the DFT/6-31G(d)

molecules	2	3	4	6	7	8
			Bond Distance (Å)			
C1−O2	1.2106	1.2111	1.3009	1.2370	1.2563	1.3094
C6−O3	1.2141	1.2909	1.1924	1.2181	1.3003	1.2291
			Bond Angles (deg)			
O1−C1−C2	117.85	117.59	121.83	115.53	117.46	120.69
O3−C6−C7	115.90	123.91	116.80	117.16	116.18	117.46
			Dihedral Angles (deg)			
C1−C2−C3−C4	−91.36	96.08	−113.58	38.52	−1.05	−48.13

Table 7. ^{1}H Experimental[a] Chemical Shifts and Calculated Absolute Shieldings (δ ppm)

	basis set/method	H_1	H_2	H_3	H_4	H_5	H_6	H_7	H_8	H_9	H_{10}	H_{11}	H_{12}	H_{13}	H_{14}	H_{15}	H_{16}
1	**B3LYP/6-31G(d) //B3LYP/6-31G(d)**	**6.69**	**6.76**	**6.75**	**7.49**	**8.30**	**4.25**	**2.89**	**3.05**	**2.07**	**1.89**	**1.58**	**6.88**	**6.84**	**6.76**	**6.83**	**6.47**
2	B3LYP/6-31+G(d,p) //B3LYP /6-31G(d)	7.67	7.67	7.55	8.31	9.74	5.09	3.64	3.73	2.73	2.47	2.29	7.52	7.63	7.67	7.61	7.29
3	B3LYP/6-31+G(d,p) //B3LYP/6-31+G(d)	7.69	7.70	7.56	8.35	9.99	5.11	3.62	3.70	2.78	2.49	2.34	7.48	7.66	7.70	7.64	7.24
4	B3LYP/6-311++G(d,p) //B3LYP/6-31+G(d)	7.45	7.43	7.26	8.12	9.61	4.82	3.40	3.51	2.59	2.28	2.17	7.32	7.44	7.43	7.47	7.02
5	B3LYP/6-311+G(2d,p) //B3LYP/6-31+G(d)	7.55	7.52	7.41	8.17	9.59	5.03	3.52	3.65	2.66	2.31	2.19	7.42	7.57	7.52	7.61	7.16
6	B3LYP/6-311+G(d,p) //B3LYP/6-311+G(d,p)	7.61	7.62	7.48	8.28	9.89	5.00	3.53	3.61	2.69	2.39	2.23	7.40	7.60	7.62	7.57	7.16
7	B3LYP/6-31+G(d,p) //B3LYP/6-31+G(d,p)	7.39	7.37	7.19	8.05	9.53	4.70	3.30	3.40	2.49	2.17	2.04	7.22	7.35	7.37	7.41	6.94
8	B3LYP/6-31+G(2d,2p) //B3LYP/6-311+G(d,p)	7.79	7.75	7.66	8.42	10.12	5.26	3.75	3.85	2.87	2.49	2.33	7.61	7.79	7.75	7.78	7.38
9	B3LYP/6-31++G(d,p) //B3LYP/6-311+G(d,p)	7.37	7.52	7.18	8.06	9.51	4.71	3.31	3.42	2.50	2.17	2.05	7.25	7.36	7.34	7.40	6.94
10	B3LYP/6-31++G(2d,p) //B3LYP/6-311+G(d,p)	7.44	7.67	7.32	8.09	9.48	4.95	3.44	3.58	2.59	2.20	2.08	7.36	7.43	7.42	7.50	7.10
11	HF/6-31G(d) //HF/6-31G(d)	7.18	7.61	7.03	7.85	4.35	4.40	2.38	2.27	1.56	2.04	1.35	7.62	7.45	7.33	7.42	7.50
12	HF/6-31+G(d,p) //HF /6-31G(d)	8.02	8.27	7.72	8.57	5.68	5.17	3.04	2.84	2.24	2.78	1.98	8.45	8.23	8.07	8.16	8.17
13	HF/6-31+G(d,p) //HF/6-31+G(d)	8.05	8.30	7.74	8.60	5.71	5.24	3.09	2.78	2.26	2.77	1.98	8.42	8.25	8.09	8.20	8.20
14	HF/6-311++G(d,p) //HF/6-31+G(d)	7.80	8.09	7.50	8.39	5.42	4.99	2.90	2.57	2.05	2.59	1.77	8.21	8.05	7.90	7.97	7.99
15	HF/6-311+G(2d,p) //HF/6-31+G(d)	7.84	8.20	7.61	8.42	5.45	5.14	3.02	2.69	2.11	2.61	1.83	8.32	8.10	7.96	8.05	8.05
16	HF/6-311+G(d,p) //HF/6-311+G(d,p)	7.80	8.25	7.72	8.76	8.04	4.74	3.11	3.60	2.60	2.40	2.41	7.92	7.98	7.93	8.02	7.69
17	**HF/6-31+G(d,p) //HF/6-31+G(d,p)**	**7.75**	**8.07**	**7.50**	**8.55**	**7.73**	**4.46**	**2.92**	**3.34**	**2.46**	**2.23**	**2.24**	**7.70**	**7.76**	**7.71**	**7.83**	**7.48**
18	HF/6-31+G(2d,2p) //HF/6-311+G(d,p)	8.12	8.42	7.88	8.87	8.28	4.96	3.34	3.78	2.78	2.50	2.51	8.10	8.14	8.09	8.19	7.92
19	HF/6-31++G(d,p) //HF/6-311+G(d,p)	7.75	8.06	7.49	8.54	7.72	4.47	2.92	3.34	2.47	2.21	2.22	7.70	7.76	7.71	7.82	7.47
20	HF/6-31++G(2d,p) //HF/6-311+G(d,p)	7.78	8.15	7.57	8.55	7.64	4.63	3.07	3.46	2.52	2.23	2.24	7.82	7.84	7.76	7.89	7.61
	experimental	7.32	7.61	7.38	7.92	6.1	4.10	2.00 to 2.40	2.00 to 2.40		1.71		7.20	7.27	7.20	7.27	7.20

[a] Experimental data from ref 28.

Table 8. ^{13}C NMR Experimental[a] Chemical Shifts and Calculated Absolute Shieldings (δ ppm)

	basis set/method	C_1	C_2	C_3	C_4	C_5	C_6	C_7	C_8	C_9	C_{10}	C_{11}	C_{12}	C_{13}	C_{14}	C_{15}	C_{16}	C_{17}	C_{18}	C_{19}
1	B3LYP/6-31G(d) //B3LYP/6-31G(d)	102.8	117.2	109.0	112.2	105.3	140.2	147.6	97.1	146.9	31.5	125.4	35.7	198.1	21.4	115.4	114.6	112.3	113.8	111.7
2	B3LYP/6-31+G(d,p) //B3LYP/6-31G(d)	103.1	116.9	108.7	111.4	106.2	142.0	149.0	97.6	148.8	31.4	128.0	34.9	200.9	20.0	115.5	115.4	112.2	114.0	111.9
3	B3LYP/6-31+G(d,p) //B3LYP/6-31+G(d)	103.1	117.4	109.1	111.7	106.3	142.4	149.4	97.8	149.6	31.2	127.9	36.1	201.8	19.7	115.9	115.8	112.6	114.3	112.1
4	B3LYP/6-311++G(d,p) //B3LYP/6-31+G(d)	121.2	137.1	127.9	130.2	122.9	161.5	169.4	113.0	168.9	41.1	147.2	50.0	224.3	31.0	134.8	134.1	131.6	133.3	130.9
5	B3LYP/6-311+G(2d,p) //B3LYP/6-31+G(d)	121.2	137.0	127.7	130.2	123.7	162.0	170.3	114.0	169.9	41.6	147.9	47.7	225.2	31.0	135.0	133.9	131.8	133.1	130.5
6	B3LYP/6-311+G(d,p) //B3LYP/6-31+G(d,p)	102.3	116.5	108.1	110.9	105.7	141.5	148.6	97.0	148.0	30.5	127.0	35.3	199.8	19.0	115.0	114.9	111.7	113.5	111.2
7	**B3LYP/6-311+G(d,p) //B3LYP/6-311+G(d,p)**	**120.4**	**136.2**	**126.9**	**129.4**	**122.3**	**160.6**	**168.5**	**112.3**	**167.2**	**40.3**	**146.6**	**46.4**	**222.2**	**30.0**	**134.0**	**133.3**	**130.8**	**132.3**	**130.0**
8	B3LYP/6-31+G(2d,2p) //B3LYP/6-311+G(d,p)	104.0	118.5	110.3	112.7	107.5	142.7	150.3	97.9	151.5	30.6	128.7	35.7	202.1	19.8	116.6	116.8	113.4	115.4	113.5
9	B3LYP/6-31++G(d,p) //B3LYP/6-311+G(d,p)	120.4	136.1	126.9	129.3	122.3	160.6	168.6	112.4	167.1	40.3	146.4	46.3	222.0	30.1	133.8	133.2	130.6	132.5	129.8
10	B3LYP/6-31++G(2d,p) //B3LYP/6-311+G(d,p)	120.5	136.0	126.7	129.3	123.0	161.4	169.5	113.1	168.1	41.2	147.0	46.9	222.8	30.3	134.0	132.6	130.5	132.4	129.5
11	HF/6-31G(d) //HF/6-31G(d)	111.8	132.1	117.1	125.3	109.6	148.2	157.1	98.5	155.5	30.3	135.4	42.1	196.3	23.7	122.3	126.5	124.6	126.9	127.5
12	HF/6-31+G(d,p) //HF/6-31G(d)	111.3	131.6	116.3	124.5	110.4	148.9	157.0	97.9	156.3	29.9	136.8	41.2	197.6	22.7	122.5	126.4	124.2	126.6	127.6
13	HF/6-31+G(d,p) //HF/6-31+G(d)	111.6	132.0	116.7	124.8	110.6	148.9	157.2	98.7	156.7	29.9	137.1	41.4	198.1	22.7	122.3	126.8	124.6	127.1	127.9
14	HF/6-311++G(d,p) //HF/6-31+G(d)	126.0	147.0	131.4	138.8	122.7	164.1	171.9	110.8	171.8	37.8	152.2	49.8	213.8	21.4	137.2	147.1	139.5	142.2	143.2
15	HF/6-311+G(2d,p) //HF/6-31+G(d)	125.7	147.1	131.3	138.9	123.6	164.9	173.3	111.6	173.2	37.9	152.9	50.6	214.8	31.9	137.3	141.9	141.9	142.4	143.1
16	HF/6-311+G(d,p) //HF/6-31+G(d,p)	110.9	131.2	115.9	125.3	111.5	148.6	159.0	96.8	156.3	29.6	138.5	36.8	201.7	25.3	126.2	125.2	122.0	124.4	121.8
17	HF/6-311+G(d,p) //HF/6-311+G(d,p)	125.3	146.2	130.5	139.4	123.7	163.7	174.1	108.7	171.4	37.0	153.2	45.4	218.3	33.9	141.2	140.2	137.0	139.4	136.4
18	**HF/6-31+G(2d,2p) //HF/6-311+G(d,p)**	**111.7**	**132.1**	**117.0**	**126.1**	**111.7**	**149.6**	**159.9**	**97.0**	**158.9**	**30.3**	**139.2**	**37.8**	**203.3**	**26.6**	**127.0**	**126.3**	**123.1**	**125.6**	**122.8**
19	HF/6-31++G(d,p) //HF/6-311+G(d,p)	125.2	146.2	130.6	139.3	123.7	163.9	173.9	108.9	171.4	37.1	153.1	45.6	218.5	33.8	141.1	140.3	137.0	139.4	136.5
20	HF/6-31++G(2d,p) //HF/6-311+G(d,p)	125.0	146.2	130.5	139.4	124.7	163.5	175.4	110.1	171.4	38.1	153.9	46.4	218.8	34.6	141.2	140.3	137.0	139.6	136.6
	experimental	116.7	131.6	125.5	126.6	122.3	153.5	175.7	103.4	167.9	35.2	140.7	47.6	207.7	31.1	127.7	128.7	126.0	128.7	127.7

[a] Experimental data from refs 28 and 29.

the $\Delta G^{o}_{(g)}$ reference state (24.46 L at 298.15 K) from 1 atm to 1 M is accomplished. The absence of imaginary frequencies verified that all structures were true minima at their respective levels of calculation.

The tautomeric equilibrium constants were calculated from the Charton method and the following equation[26] (eq 6) which is presented below:

$$pK_T = pK_{a(\text{enol model})} - pK_{a(\text{keto model})} \quad (6)$$

In this approach the pK_a values of model molecules of both keto and enol forms are used. In models of the main tautomers the possibility of proton migrations was eliminated by replacing the acidic protons with methyl groups. Ab initio, HF, and density functional geometry optimizations were performed using the Gaussian 03W software program. All geometries were taken as starting points using the HF/6-31G(d) and B3LYP/6-31G(d) geometry optimizations. The optimized structures were then used in the solution phase to determine the solvation free energies. The total energies are given in hartrees using the conversion factor 1 hartree = 2625.5 kJ·mol^{-1}.

Results and Discussion

The obtained experimental and computed data are discussed in the following manner.

Tautomerism and Acidity. Possible tautomerization along with protonation/deprotonation patterns for the studied molecules are depicted in Scheme 2.

The evaluation of spectral data of 2-hydroxy-3-(3-oxo-1-phenylbutyl)chromen-4-one are shown in Figure 3 for the pH values 1.29 and 6.95. It is seen that considerable changes are observed in the range of pH 1.29 to 6.95.

The computed thermodynamic energies and other physical parameters were obtained and are depicted in Tables 1 and 2. The ab initio computed thermal free energies ΔG, solvation free energies $\Delta G_{(sol)}$, and experimental and calculated acidity constant, pK_a, values are given in Table 3. A good correlation is observed between the theoretical (DFT B3LYP 6-31G(d)) and the experimental pK_a values for equilibrium, 2 ⇌ 3. From this comparison, the experimental results produce good agreement with theoretical data for the 1 ⇌ 2 equilibrium using the HF 6-31G(d) theory (Table 3).

Geometrical Structure. The first task for the computational work was to determine the optimized geometry of the compounds (constants listed in Table 4). Figure 5 shows the geometries obtained for the species studied, and some relevant geometric parameters are given in Tables 5 and 6 for the systems. All geometries were taken as starting points using HF/6-31G(d) and B3LYP/6-31G(d) geometry optimizations.

We show the calculated optimized structure parameters (bond lengths, bond angles, and dihedral angles) for all of the molecules. The optimization of the geometrical parameters, hence providing a structural analysis for the studied molecules, was carried out using ab initio HF/6-31G(d) and DFT with the B3LYP/6-31G(d) basis set. The stability of the optimized geometries was confirmed by frequency calculations, which give positive values for all of the obtained frequencies. When the neutral and protonated forms of the molecule are compared regarding the carbonyl bond, the bond length of the protonated carbonyl group is found to be elongated, and the nearby angles are also found to be increased.

GIAO Predictions of $^{1}H/^{13}C$ Chemical Shifts and Comparison with Experimental Results. The GIAO method with the B3LYP functional theory and HF theory with different basis sets was employed to interpret the available NMR data

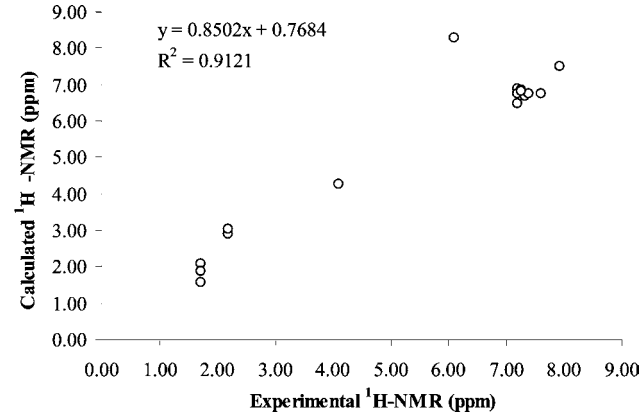

Figure 6. Comparison of experimental and theoretical ^{1}H NMR chemical shifts of warfarin as calculated at the B3LYP/6-31G(d)//B3LYP/6-31G(d) level of theory.

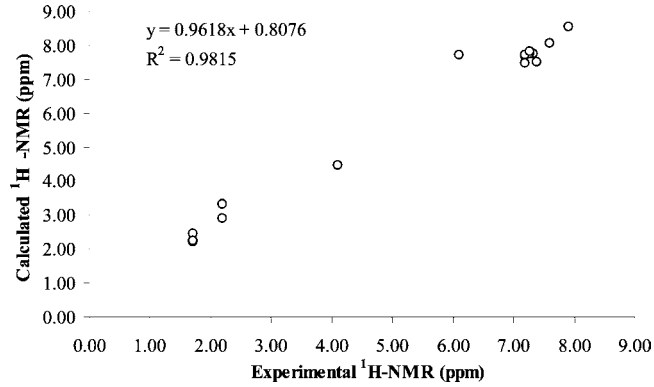

Figure 7. Comparison of experimental and theoretical ^{1}H NMR chemical shifts of warfarin as calculated at the HF/6-31+G(d,p)//HF/6-31+G(d,p) level of theory.

(chemical shifts) of warfarin. The calculated and the experimental NMR chemical shifts of warfarin are shown in Tables 7 and 8. The depicted list of the GIAO theoretical isotropic ^{1}H and ^{13}C chemical shifts are related to the TMS data obtained from HF and DFT for 2-hydroxy-3-(3-oxo-1-phenylbutyl)-chromen-4-one. Various different approaches have been developed and tested; however, the most widely used technique is the GIAO calculation of NMR chemical shifts at the DFT (DFT) B3LYP 6-311++G(2d,p) level, which is suitable for organic molecules with 100 or more atoms.[27]

All of the structures were fully optimized with the Gaussian 03 program at the B3LYP and HF methods with different basis sets (6-31G(d), 6-31+G(d), and 6-311+G(d,p)). After the optimization, ^{1}H and ^{13}C chemical shifts were calculated with the GIAO method using the corresponding TMS shielding calculated data at the same theoretical level as the reference. However, the prediction of NMR chemical shifts using any of the methods is in good agreement with experiment. To compare isotropic shieldings with experimental chemical shifts, the NMR parameters for TMS were calculated for each basis set and used as the reference molecule. The numbering systems for warfarin are shown in Figure 4.

The B3LYP-based calculation demonstrates similar agreement for the ^{1}H chemical shifts in Table 7. The data in Table 8 reveal that the HF-based calculation results are in excellent agreement with the experimental ^{13}C chemical shift data. The GIAO calculations were performed using DFT(B3LYP) with the 6-31G(d), 6-31+G(d,p), 6-311++G(d,p), 6-311+G(2d,p), 6-311+G(d,p), and 6-31G+(2d,2p) basis sets as recommended[30]

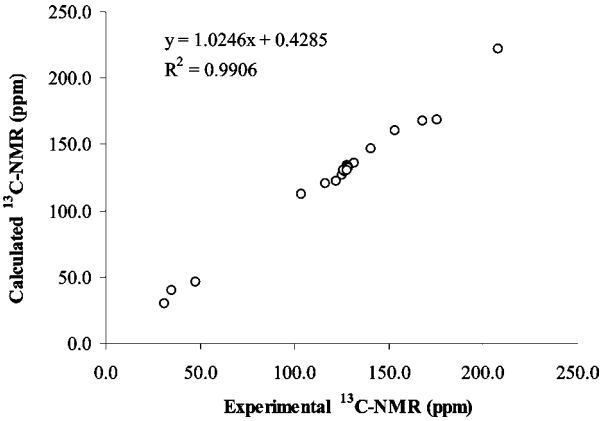

Figure 8. Comparison of experimental and theoretical ^{13}C chemical shifts of warfarin as calculated at the B3LYP/6-311+G(d,p)//B3LYP/6-311+G(d,p) level of theory.

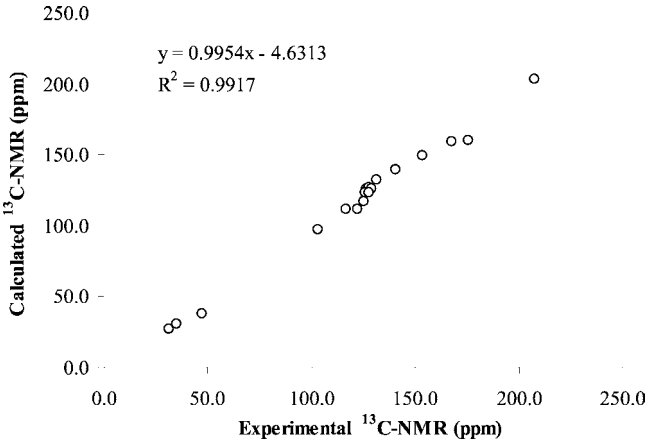

Figure 9. Comparison of experimental and theoretical ^{13}C chemical shifts of warfarin as calculated at the HF/6-31+G(2d,2p)//HF/6-311+G(d,p) level of theory.

and HF levels of theory with the same basis sets. These trends are in good agreement with experimental results.

Although linear correlations typically exist between experimental and theoretical values predicted in this manner, the slope of the line can deviate from 1, depending on the computational method and choice of basis set (Figures 6 to 9).[31–34] A linear scaling of the calculated chemical shifts is used to account for the differences in the conditions of the experimental measurements and computational predictions, as well as for possible systematic errors either at the geometry optimization or NMR stages of the calculations.

Conclusions

In this study, we have proved the feasibility of the UV−vis spectrophotometric method in the determination of the ionization constants of warfarin in EtOH−water solutions. We obtained a pK_a of 5.34 for warfarin using a UV−vis spectrophotometric technique. This result shows perfect agreement with our theoretical results, especially with the DFT/6-31G(d) calculated value of 5.40. The calculations were performed with DFT/6-31G(d) and HF/6-31G(d) using Tomasi's method. To calculate solvation energies, a popular continuum model of solvation, the CPCM, has been used at the HF and B3LYP levels of theory in conjunction with different basis sets. The theoretically obtained protonation and deprotonation constants show good agreement with the acidity constants which were experimentally determined in our present work. A reasonable correlation was obtained between the protonation/deprotonation energies of the compunds calculated at the HF/6-31G(d) and B3LYP/6-31G(d) levels of theory and their aqueous pK_a values. The ability to predict acidity using a coherent, well-defined theoretical approach, without external approximation or fitting to experimental data would be very useful to chemists. Finally, it seems that ab initio (HF and DFT) calculations of physical parameters provide satisfactory results to supplement experimental findings for quantitative structure−activity relation studies (QSAR). As we had indicated earlier in molecular geometrical studies, the bond length of the protonated carbonyl group was found to be elongated, and the nearby angles were also found to be increased.

In addition, the experimental and theoretical investigations of the 2-hydroxy-3-(3-oxo-1-phenylbutyl)chromen-4-one have been performed successfully by using NMR and quantum chemical calculations. The ^{13}C and ^{1}H chemical shifts of the optimized geometries are calculated. In this way, carbon and proton NMR spectra of 2-hydroxy-3-(3-oxo-1-phenylbutyl)-chromen-4-one have been assigned, and the experimental chemical shifts have been compared with the results of density functional calculations employing large basis sets. We now report a unique collection of experimental NMR data (chemical shifts) for 2-hydroxy-3-(3-oxo-1-phenylbutyl)chromen-4-one showing the effectiveness of GIAO/DFT and GIAO/HF calculations in predicting chemical shifts. The GIAO method using the B3LYP and HF with different basis sets were applied to 2-hydroxy-3-(3-oxo-1-phenylbutyl)chromen-4-one. The application of the GIAO method yields ^{1}H and ^{13}C chemical shifts that are in agreement with the experimental results. A comparison of the B3LYP and HF methods showed that the best results for small molecules with the HF/HF approach. For the ^{13}C shieldings, the HF/HF calculations were almost identical in quality, and for ^{1}H the B3LYP/B3LYP performed beter. The GIAO/DFT approach predicted the ^{13}C shifts of heteroaromatic ring carbons which are in better agreement with the experiment. To summarize our results, we report a general correlation between experimental and theoretical results for NMR and pK_a data. The calculated isotropic shielding constants based on DFT/GIAO and HF/GIAO methods are found to be in good agreement with the experimental results.

Acknowledgment

Our research group is greatly in debt to the Board of Scientific Research Projects of Eskişehir Osmangazi University for providing the Gaussian 03W program.

Literature Cited

(1) Kimura, R.; Miyashita, K.; Kokubo, Y.; Akaiwa, Y.; Otsubo, R.; Nagatsuka, K.; Otsuki, T.; Okayama, A.; Minematsu, K.; Naritomi, H.; Honda, S.; Tomoike, H.; Miyata, T. Genotypes of vitamin K epoxide reductase, G-Glutamyl Carboxylase and Cytochrome P450 2c9 as determinants of daily warfarin dose in Japanese Patients. *Thromb. Res.* **2007**, *120*, 181–186.

(2) O'Reilly, R. A.; Aggeler, P. M. Determinants of the response to oral anticoagulant drugs in man. *Pharmacol. Rev.* **1970**, *22* (1), 35–96.

(3) West, B. D.; Preis, S.; Schroeder, C. H.; Link, K. P. Studies on the 4-Hydroxycoumarins. XVII. The Resolution and Absolute Configuration of Warfarin. *J. Am. Chem. Soc.* **1961**, *83*, 2676–2679.

(4) Hutchinson, D.; Tomlinson, J. The structure of dicoumaral and related compounds. *Tetrahedron* **1969**, *25*, 2531–2537.

(5) Valente, E. J.; Lingafelter, E. C.; Porter, W. R.; Trager, W. F. Structure of warfarin in solution. *J. Med. Chem.* **1977**, *20*, 1489–1493.

(6) Valente, E. J.; Trager, W. F.; Jensen, L. H. The crystal and molecular structure and absolute configuration of (−)-(S)-warfarin. *Acta Crystallogr.* **1975**, *31*, 954–960.

(7) Valente, E. J.; Porter, W. R.; Trager, W. F. Conformations of selected 3-substituted 4-hydroxycoumarins in solution by nuclear magnetic resonance. Warfarin and phenprocoumon. *J. Med. Chem.* **1978**, *21*, 231–234.
(8) Giannini, D. D.; Chan, K. K.; Roberts, J. D. Carbon-13 Nuclear Magnetic Resonance Spectroscopy. Structure of the Anticoagulant Warfarin and Related Compounds in Solution. *Proc. Natl. Acad. Sci. U.S.A.* **1974**, *71*, 4221–4223.
(9) Castleberry, B.; Valente, E. J.; Eggleston, D. S. Open-cyclic warfarin isomerism: 5-hydroxywarfarin. *J. Chem. Crystallogr.* **1990**, *20*, 583–593.
(10) Valente, E. J.; Santarsiero, B. D.; Schomaker, V. Conformation of dihydropyran rings. Structures of two 3,4-dihydro-2H,5H-pyrano[3,2-c][1]benzopyran-5-ones. *J. Org. Chem.* **1979**, *44* (5), 798–802.
(11) Tam, K. Y.; Hadley, M.; Patterson, W. Multiwavelength spectrophotometric determination of acid dissociation constants Part IV. Water-insoluble pyridine derivatives. *Talanta* **1999**, *49*, 539–546.
(12) Albert, A.; Serjeant, E. P. *The Determination of Ionization Constants*; Chapman and Hall: London, 1984.
(13) Jano, I.; Hardcastle, J. C. General equation for determining the dissociation constants of polyprotic acids and bases from additive properties. Part I Theory. *Anal. Chim. Acta* **1999**, *390*, 261–266.
(14) Barbosa, J.; Barron, D.; Jimenez-Lozano, E.; Sanz-Nebot, V. Comparison between capillary electrophoresis, liquid chromatography, potentiometric and spectrophotometric techniques for evaluation of pK_a values of zwitterionic drugs in acetonitrile-water mixtures. *Anal. Chim. Acta* **2001**, *437*, 309–321.
(15) Kaliszan, R.; Haber, P.; Bączek, T.; Siluk, D. Gradient HPLC in the determination of drug lipophilicity and acidity. *Pure Appl. Chem.* **2001**, *73*, 1465–1475.
(16) Castro, G. T.; Giordano, O. S.; Blanco, S. E. Determination of the pK_a of hydroxy-benzophenones in ethanol-water mixtures. Solvent effects. *J. Mol. Spectrosc.* **2003**, *626*, 167–178.
(17) Sauerwald, N.; Schwenk, M.; Polster, J.; Bengsch, E. Spectrometric p*K* determination of daphnetin, chlorogenic acid and quercetin. *Z. Naturforsch.* **1998**, *53*, 315–321.
(18) Robinson, R. A.; Stokes, R. H. *Electrolyte Solutions, The Measurement and Interpretation of Conductance, Chemical Potential, and Diffusion in Solutions of Simple Electrolytes*, 2nd ed.; Butterworths: London, 1968.
(19) *Program CS Chem3D Ultra 10.0. Molecular Modeling and Analysis*; Cambridge Soft Corporation: Cambridge, MA, 2006.
(20) Frisch, M. J.; Trucks, G. W.; Schlegel, H. B.; Scuseria, G. E.; Robb, M. A.; Cheeseman, J. R.; Montgomery, J. A., Jr.; Vreven, T.; Kudin, K. N.; Burant, J. C.; Millam, J. M.; Iyengar, S. S.; Tomasi, J.; Barone, V.; Mennucci, B.; Cossi, M.; Scalmani, G.; Rega, N.; Petersson, G. A.; Nakatsuji, H.; Hada, M.; Ehara, M.; Toyota, K.; Fukuda, R.; Hasegawa, J.; Ishida, M.; Nakajima, T.; Honda, Y.; Kitao, O.; Nakai, H.; Klene, M.; Li, X.; Knox, J. E.; Hratchian, H. P.; Cross, J. B.; Bakken, V.; Adamo, C.; Jaramillo, J.; Gomperts, R.; Stratmann, R. E.; Yazyev, O.; Austin, A. J.; Cammi, R.; Pomelli, C.; Ochterski, J. W.; Ayala, P. Y.; Morokuma, K.; Voth, G. A.; Salvador, P.; Dannenberg, J. J.; Zakrzewski, V. G.; Dapprich, S.; Daniels, A. D.; Strain, M. C.; Farkas, O.; Malick, D. K.; Rabuck, A. D.; Raghavachari, K.; Foresman, J. B.; Ortiz, J. V.; Cui, Q.; Baboul, A. G.; Clifford, S.; Cioslowski, J.; Stefanov, B. B.; Liu, G.; Liashenko, A.; Piskorz, P.; Komaromi, I.; Martin, R. L.; Fox, D. J.; Keith, T.; Al-Laham, M. A.; Peng, C. Y.; Nanayakkara, A.; Challacombe, M.; Gill, P. M. W.; Johnson, B.; Chen, W.; Wong, M. W.; Gonzalez, C.; Pople, J. A. *Gaussian 03*; Gaussian, Inc.: Wallingford, CT, 2004.
(21) Barone, V.; Cossi, M. Quantum Calculation of Molecular Energies and Energy Gradients in Solution by a Conductor Solvent Model. *J. Phys. Chem. A* **1998**, *102* (11), 1995–2001.
(22) Wolinski, K.; Hinton, J. F.; Pulay, P. Efficient Implementation of the Gauge-Independent Atomic Orbital Method for NMR Chemical Shift Calculations. *J. Am. Chem. Soc.* **1990**, *112*, 8251–8260.
(23) Kinsella, G. K.; Rodriguez, F.; Watsona, G. W.; Rozasa, I. Computational approach to the basicity of a series of α1-adrenoceptor ligands in aqueous solution. *Bioorg. Med. Chem.* **2007**, *15*, 2850–2855.
(24) Lopez, X.; Schaefer, M.; Dejaegere, A.; Karplus, M. Theoretical evaluation of pK_a in phosphoranes: implications for phosphate ester hydrolysis. *J. Am. Chem. Soc.* **2002**, *124*, 5010–5018.
(25) Schmidt, M.; Knapp, E. Accurate pK_a determination for a heterogeneous group of organic molecules. *ChemPhysChem* **2004**, *5*, 1513–1522.
(26) Elguero, J.; Marzin, C.; Katritzky, A. R.; Linda, P. *The Tautomerism of Heterocyclic Compounds*; Academic Press: New York, 1976.
(27) Abil, E. A.; Courtier-Murias, D.; Zhou, S. Scaling factors for carbon NMR chemical shifts obtained from DFT B3LYP calculations. *J. Mol. Struct.: THEOCHEM* **2009**, *893*, 1–5.
(28) Pouchert, C. J.; Behnke, J. *The Aldrich Library of ^{13}C and ^{1}H FT NMR Spectra, 300 MHz ^{1}H/75 MHz ^{13}*; Aldrich Chemical Co.: Milwaukee, WI, 1993.
(29) Duddeck, H.; Kaiser, M. ^{13}C NMR Spectroscopy of Coumarin Derivatives. *Org. Magn. Reson.* **1982**, *20*, 55–72.
(30) Urbelis, G.; Susvilo, I.; Tumkevicius, S. Investigation of the structure of 6-amino-4-methylamino-5-nitrosopyrimidine by X-ray diffraction, NMR and molecular modeling. *J. Mol. Modell.* **2007**, *13*, 219–224.
(31) Lipowski, P.; Koll, A.; Karpfen, A.; Wolschann, P. An approach to estimate the energy of the intramolecular hydrogen bond. *Chem. Phys. Lett.* **2002**, *360*, 256–263.
(32) Forsyth, D. A.; Sebag, A. B. Computed ^{13}C NMR Chemical Shifts via Empirically Scaled GIAO Shieldings and Molecular Mechanics Geometries. Conformation and Configuration from ^{13}C Shifts. *J. Am. Chem. Soc.* **1997**, *119*, 9483–9494.
(33) Baldridge, K. K.; Siegel, J. S. Correlation of Empirical δ(TMS) and Absolute NMR Chemical Shifts Predicted by ab initio Computations. *J. Phys. Chem. A* **1999**, *103*, 4038–4042.
(34) Giesen, D. J.; Sumbulyadis, N. A hybrid quantum mechanical and empirical model for the prediction of isotropic ^{13}C shielding constants of organic molecules. *J. Chem. Phys.* **2002**, *4*, 5498–5507.

Received for review May 26, 2009. Accepted February 19, 2010.

JE900456V